contraction ratios based on a normal shock at the mass-weighted inlet Mach number ($\bar{M}_1$).

For inlets with predominately inviscid intake flow, the usual concept of contraction ratio based on normal shock losses is an upper limit for the starting criterion. This usual starting criterion also provides conservative guide lines for the starting of mixed compression inlets[3] and internal compression inlets sim lar to the type tested in the present investigation when the inlet height is generally greater than the boundary-layer thickness and the associated pressure recovery is greater than that for a normal shock. This is illustrated in Fig. 4 where experimental y obtained contraction ratios greater than those calculated for normal shock losses are shown for $\alpha_c = 4°$. The measured pressure recoveries for those started configurations were greater than those for a normal shock.

In summary, the inlet total pressure recovery resulting not merely from shock losses but from all shock and viscous losses must be considered in the starting criterion for hypersonic inlets with large turbulent boundary layers relative to the inlet height. The pressure recovery required for starting the inlets of the present investigation was reasonably well predicted by the one-dimensional analysis. The present experiments also show that the inlet pressure recovery is sensitive to many design parameters, particularly the height of the inlet relative to the boundary-layer thickness. When the inlet height is less than the boundary-layer thickness, the usual starting criterion of contraction ratio based on normal shock loss is not adequate for the inlets investigated.

References

1 Henry, J. R. et al., "Boundary Layer and Starting Problems on a Short Axisymmetric Scramjet Inlet," SP-216, 1969, NASA, pp. 481–508.

2 Shapiro, A. H., *The Dynamics and Thermodynamics of Compressible Fluid Flow*, Vol. 1, 1953, Ronald Press, New York, pp. 144–145.

3 Mitchell, G. A. and Cubbison, R. W., "An Experimental Investigation of the Restart Area Ratio of a Mach 3 Axisymmetric Mixed Compression Inlet," TMX-1547, 1968, NASA.

Method for Predicting Wing Section Pressure Distributions, Lift, and Drag in Transonic Mixed Flow

Henry A. Fitzhugh*

McDonnell Douglas Corporation, St. Louis, Mo.

The purpose of this Note is to show how several existing methods for predicting pressure on various parts of an airfoil section in transonic flow can be combined with suitable assumptions to yield the pressure distribution over the entire airfoil, from which the lift and pressure drag (excluding skin-friction drag) can be calculated. The position of the shock wave and the pressure distribution near the leading edge are both calculated. The four methods employed will be outlined only briefly here; the reader is referred to the original publications[1–3] for details.

Sinnott and Osborne[1] have formulated an empirical method for prediction of shock location and pressure distributions on an airfoil from the airfoil crest (where the tangent to the airfoil surface is parallel to the freestream) to the trailing edge. Their method relies heavily on empiricism and on a detailed understanding of the physical phenomena present in a supersonic flow region terminated by a shock wave. The Sinnott and Osborne method was used by the author in toto except that for the present results, compressibility corrections were made using the Kármán-Tsien law instead of the Prandtl-Glauert rule as used by Sinnott and Osborne.†

More recently, Thompson and Wilby[2] have given two methods which between them apply to the calculation of pressure distributions from the airfoil leading edge to the crest. The first of these methods ($TW1$) relies on an empirical relation found between an incompressible velocity distribution near the leading edge stagnation point and the compressible velocity distribution in the same region at a freestream Mach number (M_∞) between 0 and 1. Furthermore, their first formulation is valid only where the surface slope is large and only relates two flows with the same stagnation point.

To apply the $TW1$ procedure, it was necessary to devise a method for predicting the stagnation-point location in a compressible flow. In an incompressible flow, the stagnation point moves rearward as the angle of attack and lift increase. At a constant angle of attack, the stagnation point moves forward and the lift increases as the Mach number increases. In both of these situations, the lift is increasing but the stagnation point moves in opposite directions. These trends seem contradictory, but the following explanation can be offered. We note that the stagnation point for affinely related airfoils moves forward as the thickness ratio decreases and that the total lift of a specified flow system around a body depends on where the stagnation points are confined. On a wing section, the lift is increased by moving the leading edge stagnation point rearward. The similarity rule for subsonic flow tells us that an airfoil of thickness ratio τ in a freestream with Mach number M_∞ is equivalent to an airfoil in incompressible flow with a thickness of $\tau/(1 - M_\infty^2)^{1/2}$. Moreover, the Prandtl-Glauert rule tells us that the lift curve slope of a

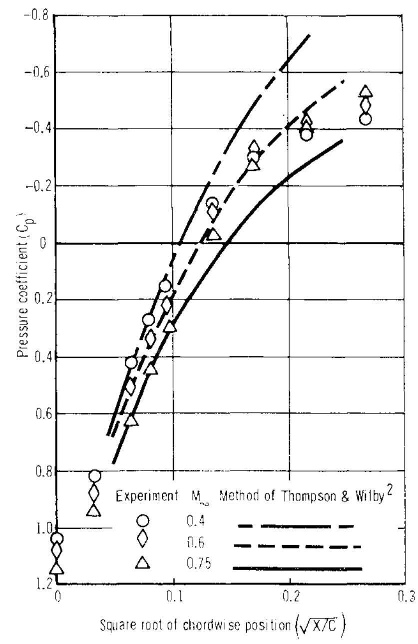

Fig. 1 Comparison of results of method of Thompson and Wilby[2] with experimental data from Ref. 4 NACA 0012 airfoil, zero angle of attack; coordinates for the NACA 0012 can be found in Ref. 6.

Received January 28, 1970. This work was conducted under the McDonnell Douglas Independent Research and Development program.

* Research Scientist, McDonnell Douglas Research Laboratories.

† The author is indebted to L. G. Niedling for programing this part of the calculations.

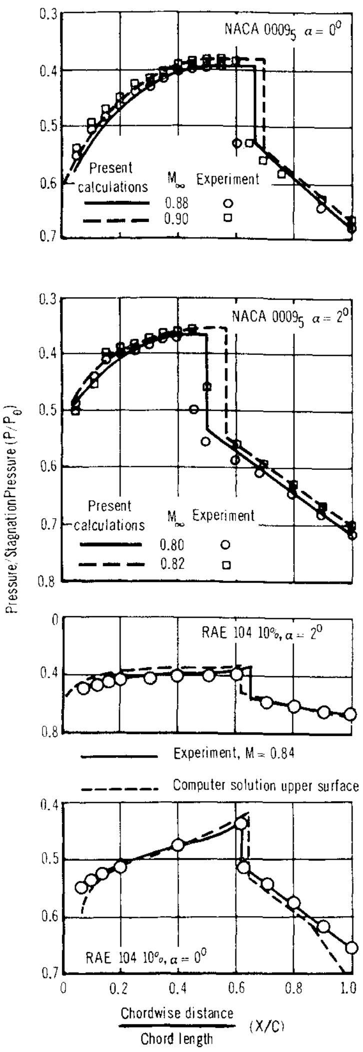

Fig. 2 Theoretical calculations compared with experiment from Ref. 1.

wing at a Mach number M_∞ is reduced by a factor of $(1 - M_\infty^2)^{1/2}$ in an incompressible flow. Thus, if we postulate that a wing section in a compressible stream can be compared to a wing in an incompressible stream by the aforementioned rules, we see that the wing in compressible flow has a smaller thickness ratio and a lower angle of attack (for the same lift) than the wing section in incompressible flow. Both of these effects will move the stagnation point forward, as is confirmed by experiment. Since for the use of the *TW*1 method near the leading edge, we need the incompressible velocity distribution with the identical stagnation point for the compressible flow calculation of a wing of the thickness ratio τ at M_∞, it seems appropriate to use the velocity distribution corresponding to a wing at Mach zero with thickness ratio $\tau/(1 - M_\infty^2)^{1/2}$ and angle of attack $\alpha/(1 - M_\infty^2)^{1/2}$. This approach is heuristic, of course, and its assumptions really can only be justified by the end results. The incompressible velocity distribution to be used in the *TW*1 procedure was calculated by the method of Theodorsen[3] which accurately predicts the velocity distribution and stagnation point on an airfoil in incompressible flow.

Figure 1 shows a comparison of the predictions of the *TW*1 theory with experiments. The pressure coefficient C_p is plotted as a function of the chordwise position X/C. Near the leading edge, the agreement is quite good, but farther back the theoretical predictions are not accurate. This disagreement may not, however, be entirely the fault of the theory; if the experimental wing were at any small incidence, instead of exactly zero, a suction peak would begin to develop near the leading edge, which would contribute to the disagreement shown in Fig. 1. In any case, it is just near the leading edge where a correct pressure distribution is most needed for the present calculations.

Table 1 Calculated lift and drag coefficients for a NACA 0008-34 airfoil compared with experimental results given in Ref. 8

		Calculated		Experiment	
M_∞	$\alpha°$	C_L	C_D	C_L	C_D
0.82	1	0.112	0.008	0.12	0.007
0.80	2	0.24	0.011	0.25	0.010
0.80	3	0.38	0.0176	0.40	0.017
0.75	4	0.44	0.033	0.45	0.020
0.78[a]	4	0.49	0.036	0.50	0.026

[a] Indicates that the boundary layer was in a state of incipient separation at the shock foot.

The second method (*TW*2) presented by Thompson and Wilby[2] is for the calculation of pressure distributions between the sonic point near the leading edge and the shock wave terminating the supersonic flow region. The *TW*2 method is restricted to a sonic stream, i.e., $M_\infty = 1$. However, as a result of the phenomenon of Mach number freeze, the pressure distribution for a high subsonic freestream will be close to that for a sonic stream.

The *TW*2 method relies on an empirical correlation between the chordwise position and the sum of the Prandtl-Meyer angle and local surface slope. There is also a constant multiplying that sum which the authors suggest may be evaluated from boundary conditions at the sonic point. This, of course, requires the knowledge of the sonic point location which is difficult to calculate. It could be found from the results of the *TW*1 method, but that would mean that the accuracy of the *TW*2 calculation would depend on the results of the *TW*1 method. Moreover, if the surface slope were not large at the sonic point, the results of the *TW*1 method calculation would be inaccurate. Therefore, for the purposes of this study, it was decided to match the pressure prediction of the *TW*2 method to the pressure predicted by the Sinnott and Osborne method at the airfoil crest, thus alleviating the problem of accurate prediction of sonic point location.

The only remaining calculation is that of the lower surface from the stagnation point to the trailing edge. The method of Theodorsen[3] was again used to predict the incompressible lower surface pressure distribution, which was then corrected for compressibility by using the Kármán-Tsien law.

Thus, by a combination of four calculation techniques the pressure on the entire surface of the airfoil can be calculated. It should be noted that we have tacitly assumed that the shock wave on the upper surface is not strong enough to separate the boundary layer. In this connection, the separation criterion of Pearcey[5] is useful. If separation occurs at the shock foot, the predictions of the Sinnott and Osborne method are invalid.

Figure 2 shows the results of calculations on an RAE 104 and NACA 0009_5 airfoil sections at different angles of attack (α). Coordinates for these airfoils can be found in Refs. 6 and 7, respectively. The experimental data do not go nearer than 5% chord to the nose, but up to that point the agreement is satisfactory.

More important, knowledge of the pressure distribution on an airfoil enables us to calculate the lift and pressure drag (by drawing a drag loop and measuring its area). Table 1 shows a comparison of calculated lift and pressure drag coefficients compared with experiment.

The results for lift coefficient show good agreement for all cases given previously whereas the drag results are good except at high angles of attack. The discrepancies in drag prediction probably result from the assumptions made about stagnation point movement at high angle of attack. The small leading edge radius of the 0008-34 airfoil only accentuates the problem. Errors in pressure prediction will affect drag predictions much more than lift predictions because leading edge suction is an important factor in resultant pressure drag.

In conclusion, it is shown that good estimates of pressure distributions can be derived from the combination of calculation procedures presented here. Also accurate lift and drag predictions can be made up to moderate angles of attack in transonic mixed flow.

References

[1] Sinnott, C. S. and Osborne, J., "Review and Extension of Transonic Aerofoil Theory," R & M 3136, 1961, British Aeronautical Research Council.

[2] Thompson, N. and Wilby, P. G., "Leading Edge Supersonic Velocity Peaks and the Determination of the Velocity Distribution on an Aerofoil in a Sonic Stream," Proceedings of AGARD Conference on Transonic Aerodynamics, AGARD C.P. 35, 1968.

[3] Theodorsen, T., "Theory of Wing Sections of Arbitrary Shape," Rept. 411, 1931, NACA.

[4] Wilby, P. G., "The Calculation of Subcritical Pressure Distributions on Symmetric Aerofoils at Zero Incidence," Rept. 1208, 1967, British National Physical Laboratory.

[5] Pearcey, H. H., "The Aerodynamic Design of Section Shapes for Swept Wings," *Advances in Aeronautical Sciences*, Vol. 3, 1960, p. 292.

[6] Pankhurst, R. C. and Squire, H. B., "Calculated Pressure Distributions for the RAE 100-104 Aerofoil Sections," TN Aero 2039, 1950, British Royal Aircraft Establishment.

[7] Abbott, I. H. and Von Doenhoff, H. E., *Theory of Wing Sections*, Dover, New York, 1959, p. 313.

[8] Antonio, F., "Completed Tabulation in the U.S. of Tests of 24 Airfoils at High Mach Numbers," ACR No. L53E21, 1945, NACA.

Severity Comparisons of Specified and Actual Impulse Tests

KENNETH A. STEAD*

University of Mississippi, University, Miss.

Introduction

MANY systems and components are required to withstand a certain impulse test, the application of several to many short term, relatively large, forces. Because of the equipment limitations, the specified impulses sometimes cannot be duplicated, and the question arises: Is the component satisfactory or not? Solutions exist for some configurations, but they tend to be sophisticated and the testing engineer may not have time to familiarize himself with them. Even more important, there are a multitude of configurations which defy analysis, for which no solutions are available. Included in the latter are bellows, valves, pipe lines with bends, etc. The exposition below develops a simple method of determining, in some cases, an absolute answer to the question, and in any case, an aid to engineering judgement.

The assumptions and limitations of the analysis are 1) maximum displacement is the basic measure of severity, and this is not always the case, but stress wave and stability solutions are rare and offer no hope of being generalized; 2) it is supposed that small, linear vibrations ensue; 3) the only differences between the specified and actual impulses are in their magnitudes and time profiles, and the test force or pressure is applied in the same place and with the same relative distribution as that specified; 4) the first few resonant frequencies have been found by experiment, applying the force in the same place as during the impulse test; 5) the specified and test impulses are periodic.

Received December 10, 1969.

* Assistant Professor, Department of Civil Engineering.

Development

For small vibrations of an elastic system, there exists[1] a set of normal generalized coordinates such that Lagrange's equations of motion reduce—in the absence of friction—to a set of uncoupled differential equations

$$q_i + P_i^2 q_i = Q_i(t)/m_i \tag{1}$$

in which q_i is the ith generalized coordinate, P_i is the natural frequency associated with the ith natural mode of vibration, Q_i is the generalized force corresponding to the ith mode, and m_i is generalized mass. For a continuous body or system there are an infinity of coordinates and, hence, an infinity of Eq. (1). As is well known, for practical purposes, only a few of the lower modes need be considered.

The forcing functions, both specified and test, are supposed to be arbitrary except for periodicity. Hence, Q_i is conveniently expressed as

$$Q_i(t) = Q_{i0}\left[a_0 + \sum_{n=1}^{\infty} (a_n \cos nz + b_n \sin nz)\right] \tag{2}$$

in which Q_{i0} is the maximum value of the generalized force Q_i; a_0, a_n, and b_n are the Fourier coefficients for a function $f(z)$ having the same time profile as the forcing function with maximum amplitude unity, and $z = \omega t = 2\pi t/T$ where ω is the frequency and T is the period of the forcing function.

Since we are dealing with many pulses, and the natural vibrations induced quickly become insignificant even with small damping, we need only the particular solution of Eq. (1). Substituting Eq. (2) into Eq. (1) and defining

$$\beta_i = \omega/P_i \tag{3}$$

the particular solution of Eq. (1) is

$$q_i = \frac{Q_{i0}}{m_i P_i^2}\left[a_0 + \sum_{n=1}^{\infty} \frac{1}{(1 - n^2\beta_i^2)} (a_n \cos nz + b_n \sin nz)\right] \tag{4}$$

The absolute maximum of (4) is desired. For most specified forcing functions, it will be clear that this maximum is attained when the series sum is either

$$[\text{sum}] = a_0 \pm \sum_{n=1}^{\infty} \frac{a_n}{(1 - n^2\beta_i^2)} \tag{5a}$$

or

$$[\text{sum}] = \pm \sum_{n=1}^{\infty} \frac{b_n}{(1 - n^2\beta_i^2)} \tag{5b}$$

This is not the case for the forcing function actually applied in the test. It is likely neither even nor odd, and the angles nz for which the series sum is a maximum not obvious. One might take d/dz of Eq. (4), equate it to zero, and solve for the angles at which the relative maxima and minima occur. Generally this will be a trial and error process requiring a series sum for each trial. It is probably less time consuming and certainly simpler to calculate the series sum for close-spaced arguments, say $\pi/18$, and take the absolute maximum found as the required sum.

Supposing the maximum absolute value of the series to be found, the maximum value of the ith coordinate, q_i is written

$$\bar{q}_i = (Q_{i0}/M_i P_i^2)\ [\text{sum}] \tag{6}$$

Denoting quantities associated with the test with superscript t and those associated with the specifications with superscript s, the ratio of the maximum value of the ith